

**Excited and ground state properties of LaSrMnO<sub>4</sub>: A combined x-ray spectroscopic study**K. Kuepper,<sup>1,2,\*</sup> R. Klingeler,<sup>3</sup> P. Reutler,<sup>3</sup> B. Büchner,<sup>3</sup> and M. Neumann<sup>2</sup><sup>1</sup>Forschungszentrum Rossendorf, Institute of Ion Beam Physics and Materials Research, P.O. Box 51 01 19, D-01314 Dresden, Germany<sup>2</sup>Department of Physics, University of Osnabrück, Barbarastrasse 7, D-49069 Osnabrück, Germany<sup>3</sup>Institute for Solid State Research IFW Dresden, P.O. Box 27 01 16, D-01171 Dresden, Germany

(Received 18 February 2006; revised manuscript received 21 June 2006; published 5 September 2006)

The electronic properties of the parent compound of the single layered manganites La<sub>1-x</sub>Sr<sub>1+x</sub>MnO<sub>4</sub>, namely LaSrMnO<sub>4</sub> have been investigated in a detailed spectroscopic study. We apply different complementary x-ray spectroscopic techniques in the soft x-ray regime. X-ray photoelectron spectroscopy and normal-like x-ray emission spectroscopy were used to reveal a detailed picture of the total and partial densities of states in this compound. Furthermore we apply resonant x-ray emission spectroscopy to the Mn *L*<sub>2,3</sub> edges. The spectra exhibit a rich multiplet structure. Resonant x-ray emission spectroscopy at the O *K* edge is used to study the local partial densities of states of the in plane and out of plane oxygen atoms. The results are discussed along available band structure calculations as well as charge transfer multiplet calculations.

DOI: [10.1103/PhysRevB.74.115103](https://doi.org/10.1103/PhysRevB.74.115103)

PACS number(s): 71.20.-b, 75.47.Lx, 78.70.En, 79.60.-i

**I. INTRODUCTION**

The perovskite manganites (La,Sr)<sub>n+1</sub>Mn<sub>n</sub>O<sub>3n+1</sub> display a remarkably rich phase diagram as a function of temperature, magnetic field, and doping that is due to the intricate interplay of charge, spin, orbital, and lattice degrees of freedom. This competition of different phases on the atomic scale has been the subject of many studies during the last years.<sup>1-4</sup> In particular, the cubic manganites La<sub>1-x</sub>Sr<sub>x</sub>MnO<sub>3</sub> and the bilayered compound La<sub>2-2x</sub>Sr<sub>1+2x</sub>Mn<sub>2</sub>O<sub>7</sub> (*n*=2) show colossal magnetoresistance (CMR).<sup>1,2,5,6</sup> In the last few years the discussion of the orbital degree of freedom is reopened for both three dimensional compounds such as La<sub>7/8</sub>Sr<sub>1/8</sub>MnO<sub>3</sub> and the single layered compound La<sub>0.5</sub>Sr<sub>1.5</sub>MnO<sub>4</sub>.<sup>7-11</sup>

However, the parent compound of the single layered manganites, namely LaSrMnO<sub>4</sub> has attracted much less attention up to now. LaSrMnO<sub>4</sub> crystallizes in the K<sub>2</sub>NiF<sub>4</sub> structure. The oxygen octahedra are elongated along the *c* axis, resulting in a strongly anisotropic crystal field (CF). Thus, in LaSrMnO<sub>4</sub>, the CF favors a ferro-orbital ordering of *d*<sub>3z<sup>2</sup>-r<sup>2</sup></sub> orbitals, which was recently studied theoretically,<sup>12,13</sup> and also experimentally by means of x-ray linear dichroism at the Mn *L* edge.<sup>9</sup> Compared to the cubic manganites LaSrMnO<sub>4</sub> also shows different magnetic properties. LaSrMnO<sub>4</sub> is an antiferromagnetic (AFM) insulator below *T*<sub>N</sub>=130 K. According to the Goodenough-Kanamori-Anderson (GKA) rules, *C*-type AFM spin order is also realized.<sup>11</sup> Up to now experimental investigations of the thermal expansion coefficient, the magnetic and the crystal structure by means of different diffraction, dilatometry and resonance techniques have been reported.<sup>10,11,14,15</sup>

As to the electronic structure of LaSrMnO<sub>4</sub>, Park carried out *first-principles* electronic structure calculations, and Wu *et al.* performed x-ray absorption spectroscopy.<sup>12,13</sup> Very recently results of a comprehensive study by means of extended x-ray absorption fine structure (EXAFS) at the Mn *K* edge have been published.<sup>16</sup> Besides XANES (x-ray absorption near edge structure) and EXAFS, the methods of x-ray emission spectroscopy (XES) and x-ray photoelectron spectroscopy (XPS) provide a tool of unique precision for the

investigation of the spatial distribution of the electron density. Very recently, Kuepper *et al.* have performed an electronic structure study by means of XPS and XES (Ref. 17).

Element and site specific resonant x-ray emission spectroscopy (RXES)<sup>18,19</sup> is another complementary powerful tool to investigate the electronic structure of transition metal compounds. The possibilities in the study of correlated systems by means of RXES go from Coulomb interactions on high energy scales over charge transfer excitations to lower excitation energies, especially regarding optical weakly accessible bands, such as *dd* transitions.<sup>20-22</sup> RXE spectra, which are obtained by tuning the excitation energy of the incoming photons across a corresponding x-ray absorption spectroscopy (XAS) spectrum often comprise two different components. On the one hand the so-called resonant inelastic x-ray scattering (RIXS) features often reflect the local electronic structure as *dd* transitions or charge transfer excitations in correlated electron systems. In RIXS, an incident photon is *inelastically* scattered and a photon of lower energy is detected with respect to that of *elastically* scattered photons. On the other hand ordinary fluorescence is also detected at constant photon energies. This process is often *normal* x-ray emission spectroscopy (NXES) and represents to a large extent the partial densities of states (PDOS). A number of RXES studies have been carried out regarding the cubic CMR manganites. Kurmaev *et al.* investigated Pr<sub>0.5</sub>Sr<sub>0.5</sub>MnO<sub>3</sub> by means of RXES at the Mn *L* edge. Later Butorin *et al.* correlated the multiplet structure of the Mn<sup>3+</sup> sublattice of La<sub>0.5</sub>Ca<sub>0.5</sub>MnO<sub>3</sub> with charge transfer multiplet calculations.<sup>23</sup> More systematic investigations over a series of samples with different dopant concentrations have been performed on La<sub>1-x</sub>Na<sub>x</sub>MnO<sub>3</sub> and La<sub>1-x</sub>Ba<sub>x</sub>Mn<sub>1-y</sub>TM<sub>y</sub>O<sub>3</sub> (TM=Co,Ni).<sup>24,25</sup> As to the layered manganites only the double layered La<sub>1.2</sub>Sr<sub>1.8</sub>Mn<sub>2</sub>O<sub>7</sub> has been probed by resonant x-ray emission at the Mn *L* edge.<sup>26</sup> On the other hand RXES on the O *K* edge is an appropriate tool to study the local partial densities of states in anisotropic materials like NaV<sub>2</sub>O<sub>5</sub> or Sr<sub>2</sub>RuO<sub>4</sub> (Refs. 27 and 28). In the present case we study the site specific contributions of the inequivalent in plane (O1) and out of plane (O2) oxygen atoms to the O *K*

RXE spectra in dependence of the excitation energy along the O  $K$  absorption edge.

We present here a detailed experimental picture of the electronic properties of LaSrMnO<sub>4</sub>, obtained by applying a number of complementary x-ray spectroscopic techniques, namely XPS, (R)XES, and XAS in the soft x-ray regime.  $3d$  transition metal compounds show strong interactions between the  $2p$  and the  $3d$  electrons, and hence  $2p$  core level spectra are dominated by the interactions between the  $2p$  hole with the valence electrons, i.e., multiplet effects. This is the case for the Mn  $L_{2,3}$  XAS, and also to a large extent, for the Mn  $2p \rightarrow 3d$  RXES process. Whereas transition metal  $2p \rightarrow 3d$  RXES spectra with excitation energies below or close to the TM  $2p_{3/2}$  threshold largely reflect the local electronic structure of the TMO<sub>6</sub> cluster, bandlike features become more important if the excitation energy is set to just above the TM  $L_3$  absorption maximum since the continuum excited normal fluorescence becomes more dominant. The interested reader is, e.g., referred to the review of de Groot.<sup>29</sup> In contrast the core hole interaction between O  $1s$  and O  $2p$  is negligible compared to the core level spin orbit coupling and consequently multiplet effects have no significant influence on the oxygen spectra. These can be described in the framework of electronic structure calculations based upon the so-called one-electron approximation. In the present work we compare our experimental x-ray spectroscopic studies with both available *ab initio* band structure calculations as well as full multiplet calculations.<sup>13,23,30</sup>

## II. EXPERIMENTAL DETAILS

A high quality LaSrMnO<sub>4</sub> single crystal was grown by the floating zone method; the details are described by Reutler *et al.*<sup>31</sup>

The XAS, XES, and RXES data experiments on LaSrMnO<sub>4</sub> were performed at room temperature at beamline 8.0.1 at the Advanced Light Source, Berkeley, California USA, using the x-ray fluorescence end station of the University of Tennessee at Knoxville.<sup>32</sup> Linearly polarized light with polarization in the horizontal plane was incident on the sample whose surface was in the vertical plane. Emission was measured along the electric vector of the incident light in the horizontal plane, that is, at a scattering angle of 90°. This geometry minimizes diffuse elastic scattering from the surface, since the Brewster angle in the soft x-ray range is usually very close to 45° so that the reflectivity for  $\vec{p}$  light is very close to zero. The light was incident at 30° to the sample normal. Photons with an energy of 500–700 eV are provided to the end station via a spherical 925 lines/mm grating monochromator. The Mn  $3d \rightarrow 2p$  and O  $2p \rightarrow 1s$  RXE spectra were obtained with a 1500 lines/mm, 10 meter radius grating. The excitation energies for the NXE spectra were set to 641.8 eV for the Mn  $L_3$  edge and to 550 eV for the O  $K$  edge. The overall resolution (beamline plus spectrometer) was set to around 0.6 eV, which can be obtained from the width of the Mn  $L_{2,3}$  elastic recombination peak at full width at half maximum (FWHM). This is an essentially better resolution than in most of the work which has been done on manganites so far. The spectra were calibrated using

a reference sample of pure Mn metal and MgO, respectively. The Mn  $2p$  and O  $1s$  x-ray absorption spectra were measured under the same experimental conditions in total electron yield mode (TEY). For the XAS experiments the instrumental resolution was set to 0.3 eV. The LaSrMnO<sub>4</sub> sample was rinsed with isopropanol in order to reduce surface contamination just before mounting it into the transfer chamber.

The XPS valence band was recorded at the Department of Physics, University of Osnabrück, Germany, using a PHI 5600CI multitechnique spectrometer with monochromatic Al  $K\alpha$  ( $h\nu=1486.6$  eV) radiation of 0.3 eV at FWHM. The overall resolution of the spectrometer is 1.5% of the pass energy of the analyzer, 0.35 eV in the present case. The spectrometer was calibrated using an Au foil as a reference sample (the binding energy of the Au  $f_{7/2}$  core level is 84.0 eV). The measurements were performed at room temperature. To get a surface free of contamination, the sample was fractured *in situ*.

## III. RESULTS AND DISCUSSION

### A. RXES on the Mn $L$ edge

The top panel of Fig. 1 displays the Mn  $L_{2,3}$  edge XA spectrum of LaSrMnO<sub>4</sub>. The Mn  $L_{2,3}$  XA spectrum, which is dominated by transitions to Mn  $3d$  states, consists of two broad multiplets due to the spin-orbit splitting of the Mn  $2p$  core hole. The Mn  $L_{2,3}$  XAS can be compared with ligand-field multiplet calculations for Mn<sup>3+</sup> in  $D_{4h}$  crystal symmetry.<sup>33</sup> However, quite good agreement is achieved with recently reported model calculations based upon a (MnO<sub>6</sub>)<sup>10-</sup> charge transfer cluster model in  $D_{4h}$  symmetry,<sup>30</sup> assuming a ground state configuration comprising 73.6%  $3d^4$  states and 26.4%  $3d^5\bar{L}$  charge transfer states. This calculation has been fitted to experiments on LaMnO<sub>3</sub> (Ref. 34), and one can conclude that the Mn  $L_{2,3}$  XAS of LaMnO<sub>3</sub> and LaSrMnO<sub>4</sub> are quite similar.

In the bottom panel we present the resonant Mn  $L_{2,3}$  edge x-ray emission spectra excited across the Mn  $L_{2,3}$  absorption. Labels A–I correspond to the excitation energies as marked in the XA spectrum. The RXE spectra depend strongly on the incident photon energy. The emission spectra corresponding to excitation energies A–E consist of three main resonant features, namely the elastic recombination peak and RIXS-like loss features, which appear at constant energy (about 2.2 eV and 6–9 eV) below to the elastic recombination peak. At higher excitation energies above the Mn  $L_3$  threshold (from excitation energy E) the emission spectra contain more nonresonant features which contribute to the spectra as dispersing features compared to spectra taken at incident photon energies which are below and at the Mn  $L_3$  XAS edge. If the excitation energy is increased to the Mn  $L_2$  edge, the elastic peak almost disappears while the loss feature located 2.2 eV below the recombination peak shows a strong resonance. Also the charge transfer excitations appear, while one can investigate normal fluorescence due to transitions from the Mn  $3d$  states to the Mn  $2p_{3/2}$  level about 12–14 eV below the elastic peak.

In Fig. 2 we compare the Mn  $L_{2,3}$  RXE spectra with available Mn<sup>3+</sup> charge transfer multiplet calculations,<sup>23</sup> the values

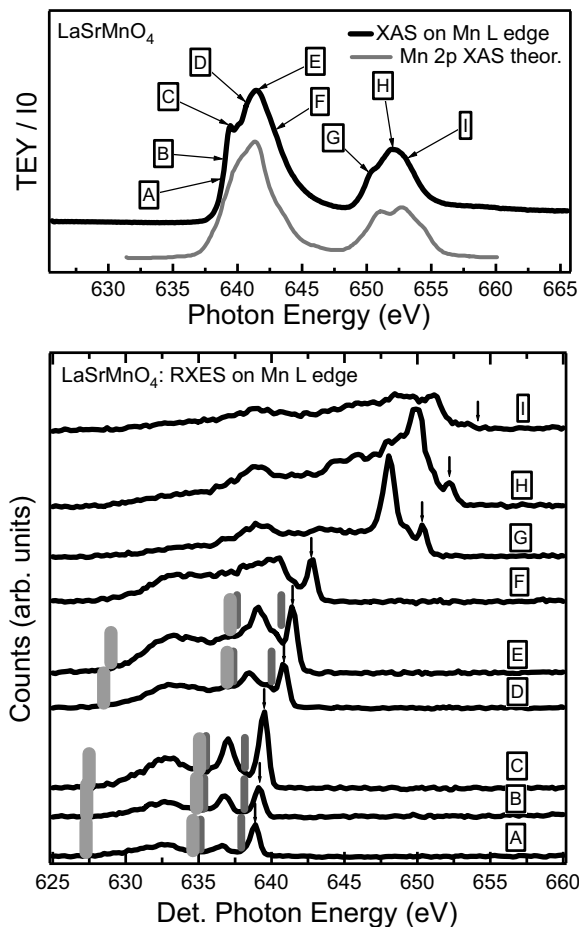


FIG. 1. Upper panel: Mn  $L$  edge XAS of  $\text{LaSrMnO}_4$  in comparison with charge transfer cluster calculations from Taguchi and Altarelli (Ref. 30). Lower panel: Mn  $L_{2,3}$  RXE spectra recorded at different excitation energies across the Mn  $L_{2,3}$  absorption edges. The excitation energies are those labeled A–I in the XAS (upper panel): A: 639.3 eV, B: 639.5 eV, C: 639.8 eV, D: 641.2 eV, E: 641.8 eV, F: 643.1 eV, G: 650.7 eV, H: 652.4 eV, I: 653.4 eV. The excitation energies are marked by arrows, the  $dd$  transitions by dark gray bars, and the charge transfer features by bright gray bars, respectively.

of the lifetime broadening of the intermediate state were estimated 0.4 eV at the Mn  $L_2$  edge and 0.6 eV at the Mn  $L_3$  edge, respectively. This comparison is somewhat limited by the fact that the multiplet calculations shown here have been performed for an almost cubic manganite applying very small values for  $D_s$  and  $D_t$ ,<sup>23</sup> whereas  $\text{LaSrMnO}_4$  is strongly distorted along the  $z$  axis. On the other hand the same calculations have been used to analyze the Mn  $L_{2,3}$  RXES of another layered manganite, namely  $\text{La}_{1.2}\text{Sr}_{1.8}\text{Mn}_2\text{O}_7$  (Ref. 26), and the simulations reproduce the RXES spectra of  $\text{LaSrMnO}_4$  rather well.

According to the calculation and earlier experimental results obtained on perovskite manganites<sup>24,25</sup> the multiplet structures located around 2.2 eV and 6–9 eV below the elastic recombination peak can be described as local  $dd$  transitions and O  $2p \rightarrow \text{Mn}3d$  charge transfer excitations, respectively. We want to point out that the present Mn  $L_{2,3}$  RXE spectra do not have such a high resolution as very recently

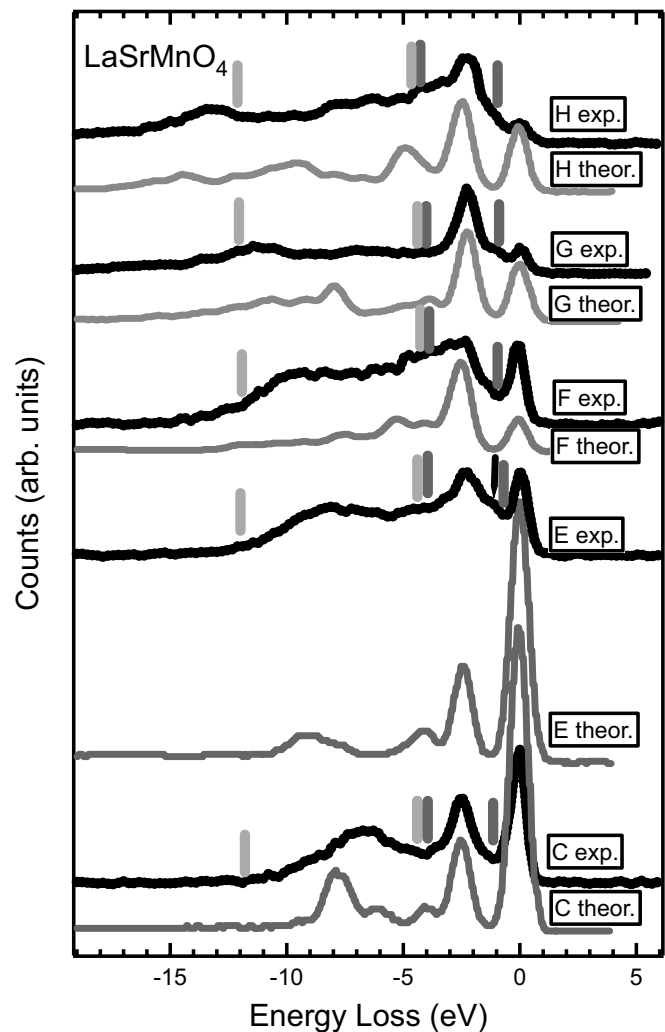


FIG. 2. The Mn  $L_{2,3}$  RXE spectra, brought to an energy loss scale and in comparison with corresponding  $\text{Mn}^{3+}$  charge transfer multiplet calculations which have been adapted from Butorin *et al.* (Ref. 23).

published data on MnO (Ref. 35). However, the signal to noise ratio is somewhat better in this work and it is of particular importance to extract spectral features at lower excitation energies (A–C). In the spectra C–E presented here also two weaker features located around 4 eV and 5.5 eV below the elastic recombination peak are nicely visible, with an overall spectral resolution essentially below 1 eV and a good signal to noise ratio. The 2.2 eV loss peak is also present at excitation energy E, corresponding to the maximum of the Mn  $L_3$  absorption. For this energy and those recorded at higher excitation energies the excitonic states begin to overlap with the ordinary Mn  $3d \rightarrow 2p$  emission, representing at least in part the occupied density of states. In addition, a further weak peak around 1.2 eV occurs if the excitation energy is set close to or to the Mn  $L_3$  XAS intensity maximum (marked with an arrow in Fig. 2). This feature is only very weak or even not present in the cluster calculations and we associate this feature with more bandlike transitions, mainly arising from the Mn  $e_g$  electrons (see Sec. III B for a more detailed discussion).

There are some other differences in detail. The elastic peak is overestimated in the calculations. The elastic recombination peak comprises several components. As indicated in Sec. II there is some scattering which comes from the surface roughness. Moreover, for excitation energies close to resonance, the dielectric constants of the sample change rapidly, what might, e.g., have influence on the Brewster angle and subsequently to the elastic peak. Finally, a number of other phenomena may occur at resonancelike quasielastic scattering. In spectrum F the intensity of the charge transfer shows a resonance. This is partly reproducible by the multiplet calculations, but also here quite strong bandlike features are overlapping the multiplet structure due to the continuum excited normal fluorescence which becomes much more important from excitation energy  $E$  on. Since we investigate a system with a strong anisotropic crystal field around the  $\text{Mn}^{3+}$  ions the scattering geometry can also have some influence on the weight of the spectral features. This has been very recently shown on  $\text{NaV}_2\text{O}_5$  (Ref. 36). The above mentioned phenomena can be investigated by angle resolved measurements or the use of variable polarization beamlines, which is beyond the scope of this work.

### B. XPS valence band and NXES

In Fig. 3 we show the XPS valence band of  $\text{LaSrMnO}_4$  (top panel), the  $\text{Mn } L_3$  (middle panel), and  $\text{O } K$  XES (bottom panel) results along with results of available LSDA +  $U$  ( $U_{\text{eff}} = 2 \text{ eV}$ ) electronic structure calculations.<sup>13</sup> In a very recent work we compared the valence band of  $\text{LaSrMnO}_4$  with a number of available electronic structure calculations,<sup>12,13</sup> and found the quite moderate  $U = 2 \text{ eV}$  value to be in the best agreement with the experiment.<sup>17</sup> Such moderate values for the onsite correlation potential have been reported also for  $\text{LaMnO}_3$ , e.g.,  $U = 2 \text{ eV}$  by Sawada *et al.*<sup>37</sup> Ravindran *et al.* performed calculations using the full-potential linearized augmented plane-wave method without invoking any special treatment of the intra-atomic correlation beyond the conventional generalized gradient approximation (GGA).<sup>38</sup> On the other side much larger values were under discussion such as  $U = 8 \text{ eV}$  in the work of Medvedeva *et al.*<sup>39</sup> According to earlier findings we compare the results presented here with the mentioned  $U = 2 \text{ eV}$  calculation.<sup>13,17</sup>

The XPS valence band consists of four distinct peaks labeled (i)–(iv). A quite weak band (i) is located just below Fermi level. A shoulder with increasing intensity (ii) is located at a binding energy of around 2 eV, followed by an absolute maximum in intensity at 4 eV (iii), and finally a local maximum between 6–7 eV (iv) on the binding energy scale.

The  $\text{Mn } L_3$  and  $\text{O } K$  XE spectra, which have been converted to the binding energy scale by using the corresponding XPS core level binding energies, are an experimental support for the identification of the XPS features. Besides the elastic recombination peak (as described in Sec. III A), the  $\text{Mn } L_3$  (R)XES is dominated by an intense spectral feature at 2 eV, furthermore shoulders at 0.7 eV and 4–5 eV are visible, followed by a second broad peak ( $\approx 8$ –10 eV). The

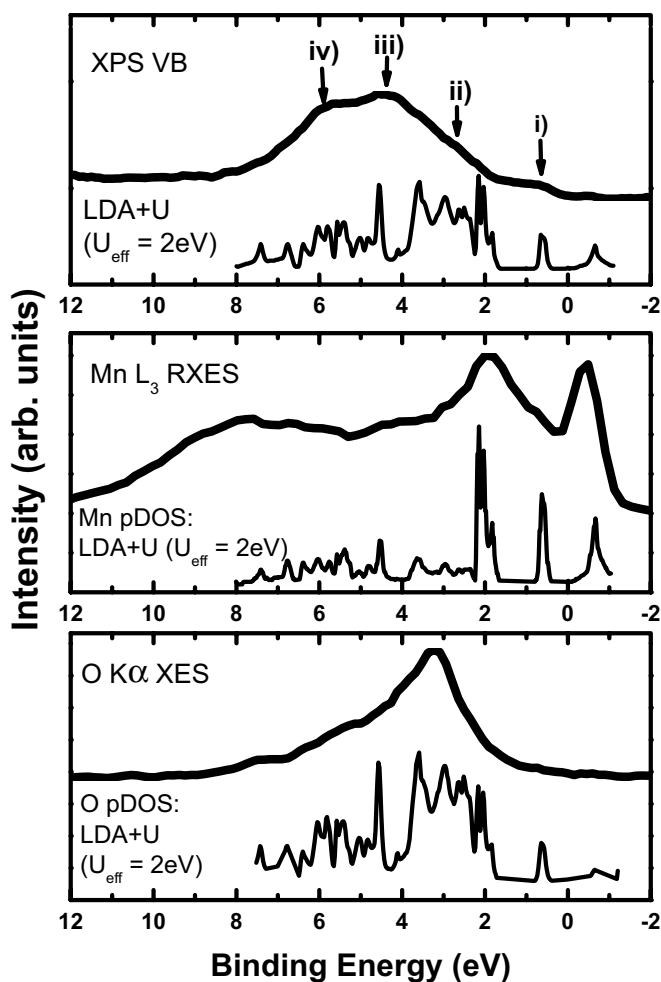


FIG. 3. The XPS valence band and XE spectra taken at the  $\text{Mn } L_3$  (spectrum  $E$  in Fig. 1) and the  $\text{O } K$  edges of  $\text{LaSrMnO}_4$ . The calculated densities of states have been extracted from Park (Ref. 13).

$\text{O } K$  x-ray emission spectrum spans the energy range from 1 eV to about 7 eV, with a rather sharp intensity maximum at 3 eV. With the help of the experimental x-ray emission and the corresponding calculated  $\text{Mn } 3d$  and  $\text{O } 2p$  partial densities of states we now can identify the features in the XPS valence band. According to the band structure calculation band (i) can be assigned to  $\text{Mn } e_g$  states, also the  $\text{Mn } L_3$  (R)XES shows a corresponding feature.<sup>12,13</sup> According to the theory and the  $\text{Mn}$  RXE spectrum the shoulder at  $\approx 2 \text{ eV}$  comprises the main part of the  $\text{Mn } t_{2g}$  orbitals, also  $\text{O } 2p$  states are present, likely energetically overlapping the  $\text{Mn } 3d$  contributions. Finally bands (iii) and (iv) are built up out of  $\text{Mn } 3d$  and  $\text{O } 2p$  states are present, which are hybridized via charge transfer.

In the lower part of the valence band [bands (iii) and (iv)] there are also a few likely  $\text{La } 4d$  and  $\text{Sr } 4p$  states present, such as, e.g., in  $\text{LaMnO}_3$  or  $\text{Sr}_2\text{FeMoO}_6$  (Refs. 25, 38, and 40) having some influence on the XPS valence band due to their large photoionization cross section. The remaining differences between the  $\text{Mn } L_3$  (R)XES and the calculated  $\text{Mn}$  PDOS can be explained by the remaining multiplet effects in the experimental spectrum.

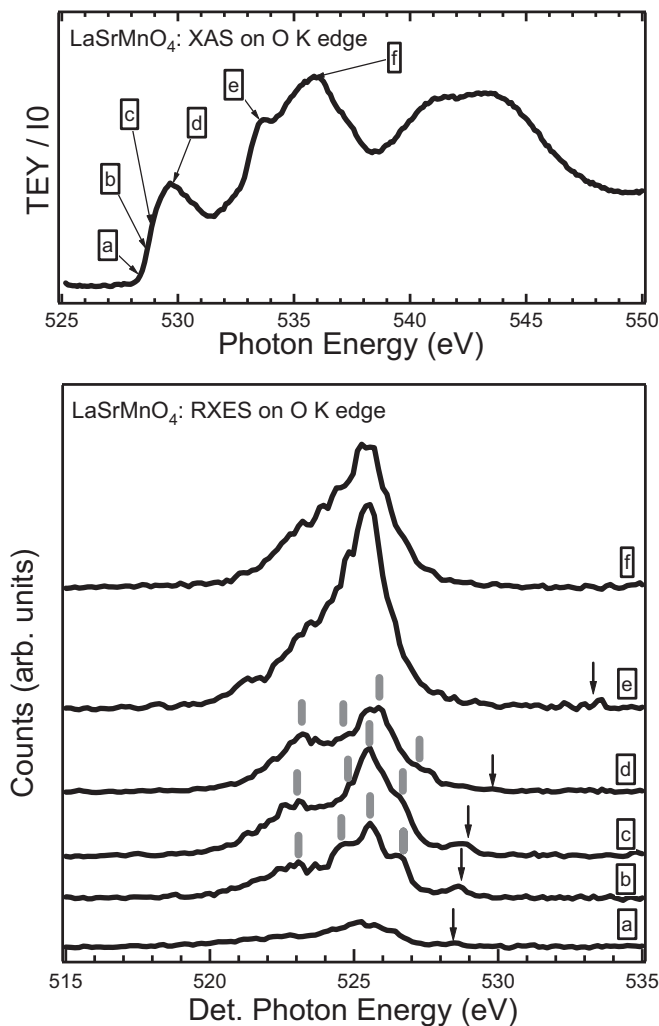


FIG. 4. Resonant x-ray emission spectra of  $\text{LaSrMnO}_4$  at the  $\text{O K}$  edge. The excitation energies are those labeled  $a-f$  in the corresponding XA spectrum (upper panel):  $a$ : 528.3 eV,  $b$ : 528.6 eV,  $c$ : 528.8 eV,  $d$ : 529.8 eV,  $e$ : 533.6 eV,  $f$ : 535.8 eV. The four peak structure (see text) is marked with bars.

#### RXES on the $\text{O K}$ edge

In the following we want to discuss the  $\text{O K}$  RXES which also show rather strong dependence on the excitation energy (Fig. 4). RXE spectra have been recorded at several excitation energies across the corresponding  $\text{O K}$  spectrum, labeled with  $a-f$ . In the lower panel of Fig. 4 the excitation energies are indicated by arrows. At lowest excitation energy  $a$  the XES spectrum looks like an approximate 6 eV broad peak with an asymmetric tail to lower photon energies (see also Fig. 5). At slightly higher excitation energies ( $b$  and  $c$ ) the shape of the RXE spectra changes significantly. These spectra show a four peak structure, a shoulder located 1.5 eV below the small elastic recombination peak, followed by an intense and rather narrow main peak. Another small shoulder is present at lower photon energies, finally a second peak around 5 eV below the elastic recombination peak appears.

The excitation energy dependence can be associated with site specific contributions from the different oxygen sites in  $\text{LaSrMnO}_4$ , namely the in-plane, or equatorial  $\text{O1}$  site, and

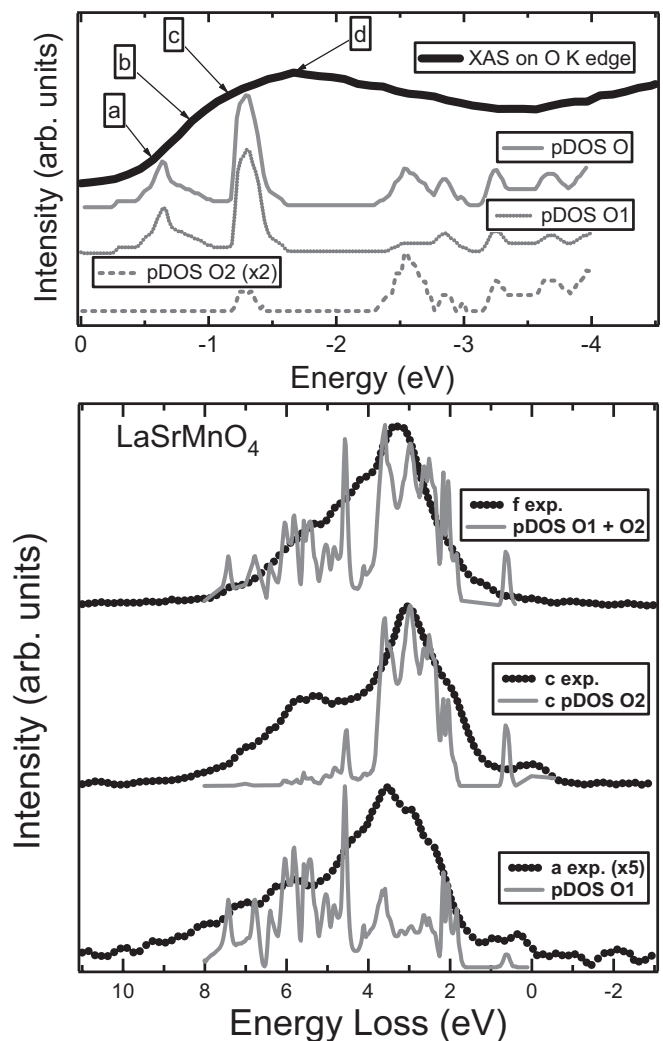


FIG. 5. Upper panel: The  $\text{O K}$  XAS of  $\text{LaSrMnO}_4$  has been brought to a common energy scale with the electronic structure calculations of Park for comparison Ref. 13. Lower panel: Selected  $\text{O K}$  RXE spectra are compared with the calculated occupied oxygen densities of states. Spectrum  $a$  is compared with the in plane ( $\text{O1}$ ) PDOS, spectrum  $c$  with the out of plane ( $\text{O2}$ ) PDOS, and spectrum  $f$  with the summarized ( $\text{O1}+\text{O2}$ ) PDOS.

the out of plane, or apical  $\text{O2}$  site. Similar effects have been observed in a few previous works dealing with other highly anisotropic materials as  $\text{Sr}_2\text{RuO}_4$  or  $\text{NaV}_2\text{O}_5$ .<sup>27,28</sup> On the other side no such energy dependence of the  $\text{O K}$  RXES in materials showing cubic symmetry has been found.<sup>28,41</sup> In order to reveal more detailed information from the resonant  $\text{O K}\alpha$  RXE spectra we compare our experimental results with the calculated local partial densities of states (LPDOS) of the in-plane ( $\text{O1}$ ) and out of plane ( $\text{O2}$ ) oxygen atoms.<sup>13</sup> Figure 5 displays a comparison of selected experimental RXE spectra with the  $\text{O1}$  LPDOS, the  $\text{O2}$  LPDOS, and finally the summarized ( $\text{O1}+\text{O2}$ ) oxygen PDOS. In the top panel a comparison of the corresponding  $\text{O K}$  XAS with the calculated unoccupied densities of states is shown.

At higher excitation energies ( $e$  and  $f$ ) both, the  $\text{O1}$  and the  $\text{O2}$  oxygen sites contribute equally to the emission spectra and we note a quite good coincidence between the calcu-

lated overall O PDOS and the experimental spectra (spectrum *f* and the corresponding calculation in Fig. 5). Above energy *b* the incoming x-ray photons are also excited into the unoccupied states, the out of plane or apical O2 sites, hence one can expect a strong resonance in the RXE spectra taken at these energies. Therefore the strong enhancement of the narrow peak located at 3 eV can be observed. As to RXE-spectrum *c*, both the shoulder at around 1.5 eV binding energy as well as the narrow but intense main peak located at 3 eV are well reproduced by theory. The shoulder at 5–6 eV can be associated with remaining transitions from O1 unoccupied sites since at this energy both oxygen sites are excited. According to theory the apical O2 atoms do not contribute to this region of the occupied DOS whereas for the O1 atoms a strong local intensity maximum is predicted.<sup>13</sup> As in a lot of layered perovskites as cuprates and other manganites this can be understood as being due to strong charge transfer effects arising from Mn 3*d* and O 2*p* states coming from the in-plane O1 atoms. At the lower excitation energy *a* only excitations from the O 1*s* states into unoccupied O1 states occur. Nevertheless the agreement between the calculated O1 LPDOS and the RXES spectrum corresponding to excitation energy *a* is much less satisfactory than for the O2 LPDOS or the oxygen PDOS (bottom spectrum in Fig. 5). The shoulder around 5–6 eV is pronounced rather intensely but not as much as suggested by theory indicating that there are already significant O2 contributions in the emission spectrum. A similar behavior has been investigated before.<sup>24,28</sup> An interesting onset for an explanation has been given by Woods *et al.*<sup>27</sup> who found that under these resonant conditions different spatial symmetries can be enhanced and suppressed not only on excitation energy dependence but also on the orientation of the polarization vector of the incoming x-ray photons. From an experimental point of view further investigation making use of polarization dependence on an oriented piece of single crystal would be desirable. From a theoretical point of view the analysis by means of a calculation taking explicitly into account the framework of the second order Kramers-Heisenberg relation, and the intra- and interatomic correlation effect has been proposed.<sup>19</sup> With such a calculation in combination with the above proposed extension of the experiment presented here perhaps one could get more detailed information on this yet not fully understood RIXS process at excitation energies very close to or below the O 1*s* absorption threshold in 3*d* transition metal compounds.

#### IV. CONCLUSIONS

In summary we have presented a combined x-ray spectroscopic study of the single layer manganite LaSrMnO<sub>4</sub> leading to a number of results. RXE spectra recorded at the Mn *L*<sub>2,3</sub> edges with a quite high resolution of 0.6 eV compared to some previous work exhibits a rich multiplet structure. The spectra consist of three main features, which can be associated with the elastic recombination peak and two loss features. The peak located around 2.2 eV below the elastic peak can be associated with a local Mn *dd* transition in agreement with multiplet calculations,<sup>23</sup> the second main feature around 6–9 eV below the elastic peak can be assigned to charge transfer transitions. Further fine structures predicted by theory are nicely resolved in the present experiment. If the excitation energy is tuned just above the Mn *L*<sub>3</sub> XAS maximum or to higher energies the spectra represent parts of the joint DOS, with the states projected on the Mn site. Regarding the valence band, by comparing the XPS valence band and complementary XES spectra reflecting the Mn 3*d* and O 2*p* partial densities of states with electronic structure calculations we find the features close to the Fermi energy and at 2 eV to be due to Mn *e<sub>g</sub>* and rather localized Mn 3*dt<sub>2g</sub>* states. The lower lying features are due to O 2*p*, strongly overlapping with Mn 3*d* and La 4*d* states. Regarding the valence band, the experimental results are in good agreement with a full-potential linearized augmented plane-wave method–local density approximation (FLAPW-LDA) + *U* calculation invoking a quite moderate effective Coulomb potential *U*=2 eV for the Mn 3*d* states.<sup>13</sup> As to the RXES performed at the O *K* edge we were able to resolve excitation energy dependent features which we could attribute to some extent to the site specific LPDOS of the inequivalent in plane (O1) and out of plane (O2) oxygen atoms. Whereas a very good coincidence between experiment and theory is achieved in the case of the oxygen (O1+O2) PDOS and the contributions of the out of plane (O2) LPDOS, less in agreement for the in-plane (O1) oxygen atoms is found. Regarding this point further experimental and theoretical efforts are necessary in the future.

#### ACKNOWLEDGMENTS

Financial support of the Ph.D. program of the federal state of Lower Saxony, Germany is gratefully acknowledged. Most of the present work has been performed at the Advanced Light Source (A.L.S.) which is supported by the U.S. Department of Energy under Contract No. DE-AC03-76SF00098.

\*Electronic address: k.kuepper@fz-rossendorf.de

<sup>1</sup>A. J. Millis, *Nature* (London) **392**, 147 (1998).

<sup>2</sup>Y. Tokura and N. Nagaosa, *Science* **288**, 462 (2000).

<sup>3</sup>M. B. Salamon and M. Jaime, *Rev. Mod. Phys.* **73**, 583 (2001).

<sup>4</sup>Y. D. Chuang, A. D. Gromko, D. S. Dessau, T. Kimura, and Y. Tokura, *Science* **292**, 1509 (2001).

<sup>5</sup>R. von Helmolt, J. Wecker, B. Holzapfel, L. Schultz, and K. Samwer, *Phys. Rev. Lett.* **71**, 2331 (1993).

<sup>6</sup>Y. Moritomo, A. Asamitsu, H. Kuwahara, and Y. Tokura, *Nature* (London) **380**, 141 (1996).

<sup>7</sup>K. Kuepper, F. Bondino, K. C. Prince, M. Zangrando, M. Zacchigna, A. F. Takács, T. Crainic, M. Matteucci, F. Parmigiani, V. R.

- Galakhov, Y. M. Mukovskii *et al.*, *J. Phys. Chem. B* **109**, 15667 (2005).
- <sup>8</sup>J. Geck, P. Wochner, D. Bruns, B. Büchner, U. Gebhardt, S. Kiele, P. Reutler, and A. Revcolevschi, *Phys. Rev. B* **69**, 104413 (2004).
- <sup>9</sup>D. Huang, W. Wu, G. Guo, H.-J. Lin, T. Hou, C. F. Chang, C. Chen, A. Fujimori, T. Kimura, H. Huang *et al.*, *Phys. Rev. Lett.* **92**, 087202 (2004).
- <sup>10</sup>R. Klingeler, D. Bruns, C. Baumann, P. Reutler, A. Revcolevschi, and B. Büchner, *J. Magn. Magn. Mater.* **290-291**, 944 (2005).
- <sup>11</sup>D. Senff, P. Reutler, M. Braden, O. Friedt, D. Bruns, A. Cousson, F. Bourée, M. Merz, B. Büchner, and A. Revcolevschi, *Phys. Rev. B* **71**, 024425 (2005).
- <sup>12</sup>W. Wu, D. J. Huang, G. Guo, H.-J. Lin, T. Hou, C. F. Chang, C. Chen, A. Fujimori, T. Kimura, H. Huang *et al.*, *J. Electron Spectrosc. Relat. Phenom.* **137-140**, 641 (2004).
- <sup>13</sup>K. T. Park, *J. Phys.: Condens. Matter* **13**, 9231 (2001).
- <sup>14</sup>S. Larochelle, A. Mehta, L. Lu, P. K. Mang, O. P. Vajk, N. Kaneko, J. W. Lynn, L. Zhou, and M. Greven, *Phys. Rev. B* **71**, 024435 (2005).
- <sup>15</sup>C. Baumann, G. Allodi, A. Amato, B. Büchner, D. Cattani, R. de Renzi, R. Klingeler, P. Reutler, and A. Revcolevschi, *Physica B* **374**, 83 (2006).
- <sup>16</sup>J. Herrero-Martín, J. García, G. Subías, J. Blasco, and M. C. Sánchez, *Phys. Rev. B* **72**, 085106 (2005).
- <sup>17</sup>K. Kuepper, R. Klingeler, P. Reutler, B. Büchner, and M. Neumann, *J. Appl. Phys.* **99**, 08Q308 (2006).
- <sup>18</sup>J. A. Carlisle, E. L. Shirley, E. A. Hudson, L. J. Terminello, T. A. Callcott, J. J. Jia, D. L. Ederer, R. C. C. Perera, and F. J. Himpsel, *Phys. Rev. Lett.* **74**, 1234 (1995).
- <sup>19</sup>A. Kotani and S. Shin, *Rev. Mod. Phys.* **73**, 203 (2001).
- <sup>20</sup>S. M. Butorin, J.-H. Guo, M. Magnuson, P. Kuiper, and J. Nordgren, *Phys. Rev. B* **54**, 4405 (1996).
- <sup>21</sup>L. C. Duda, J. Nordgren, G. Dräger, S. Bocharov, and T. Kirchner, *J. Electron Spectrosc. Relat. Phenom.* **110-111**, 275 (2000).
- <sup>22</sup>G. P. Zhang, T. A. Callcott, G. T. Woods, L. Lin, B. Sales, D. Mandrus, and J. He, *Phys. Rev. Lett.* **88**, 077401 (2002).
- <sup>23</sup>S. M. Butorin, C. Sâthe, F. Saalem, J. Nordgren, and X.-M. Zhu, *Surf. Rev. Lett.* **9**, 989 (2002).
- <sup>24</sup>F. Bondino, M. Platé, M. Zangrando, D. Cocco, A. Comin, I. Alessandri, L. Malavasi, and F. Parmigiani, *J. Phys. Chem. B* **108**, 4018 (2004).
- <sup>25</sup>K. Kuepper, M. C. Falub, K. C. Prince, V. R. Galakhov, I. O. Troyanchuk, S. G. Chiuzbăian, M. Matteucci, D. Wett, R. Szargan, N. A. Ovechkina *et al.*, *J. Phys. Chem. B* **109**, 9354 (2000).
- <sup>26</sup>A. Agui, S. M. Butorin, T. Käämbre, C. Sathe, T. Saitoh, Y. Morimoto, and J. Nordgren, *J. Phys. Soc. Jpn.* **74**, 1772 (2005).
- <sup>27</sup>G. T. Woods, G. P. Zhang, T. A. Callcott, L. Lin, G. S. Chang, B. Sales, D. Mandrus, and J. He, *Phys. Rev. B* **65**, 165108 (2002).
- <sup>28</sup>E. Z. Kurmaev, S. Stadler, D. L. Ederer, Y. Harada, S. Shin, M. M. Grush, T. A. Callcott, R. C. C. Pereira, D. A. Zatsepin, N. Ovechkina *et al.*, *Phys. Rev. B* **57**, 1558 (1998).
- <sup>29</sup>F. M. F. de Groot, *Chem. Rev. (Washington, D.C.)* **101**, 1779 (2001).
- <sup>30</sup>M. Taguchi and M. Altarelli, *Surf. Rev. Lett.* **9**, 1167 (2002).
- <sup>31</sup>P. Reutler, O. Friedt, B. Büchner, M. Braden, and A. Revcolevschi, *J. Cryst. Growth* **249**, 222 (2003).
- <sup>32</sup>J. J. Jia, T. A. Callcott, J. Yurkas, A. W. Ellis, F. J. Himpsel, M. G. Samant, G. Stöhr, D. L. Ederer, J. A. Carlisle, E. A. Hudson *et al.*, *Rev. Sci. Instrum.* **66**, 1394 (1995).
- <sup>33</sup>C. W. M. Castleton and M. Altarelli, *Phys. Rev. B* **62**, 1033 (2000).
- <sup>34</sup>J.-H. Park, S.-W. Cheong, and C. T. Chen, *Phys. Rev. B* **55**, 11072 (1997).
- <sup>35</sup>G. Ghiringhelli, M. Matsubara, C. Dallera, F. Fracassi, A. Tagliaferri, N. B. Brookes, A. Kotani, and L. Braicovich, *Phys. Rev. B* **73**, 035111 (2006).
- <sup>36</sup>G. P. Zhang and T. A. Callcott, *Phys. Rev. B* **73**, 125102 (2006).
- <sup>37</sup>H. Sawada, Y. Morikawa, K. Terakura, and N. Hamada, *Phys. Rev. B* **56**, 12154 (1997).
- <sup>38</sup>P. Ravindran, A. Kjekshus, H. Fjellvåg, A. Delin, and O. Eriksson, *Phys. Rev. B* **65**, 064445 (2002).
- <sup>39</sup>J. E. Medvedeva, M. A. Korotin, V. I. Anisimov, and A. J. Freeman, *Phys. Rev. B* **65**, 172413 (2002).
- <sup>40</sup>K. Kuepper, M. Kadiroğlu, A. V. Postnikov, K. C. Prince, M. Matteucci, V. R. Galakhov, H. Hesse, G. Borstel, and M. Neumann, *J. Phys.: Condens. Matter* **17**, 4309 (2005).
- <sup>41</sup>K. C. Prince, M. Matteucci, K. Kuepper, S. G. Chiuzbăian, S. Bartkowski, and M. Neumann, *Phys. Rev. B* **71**, 085102 (2005).